Available online at www.sciencedirect.com
ScienceDirect
Carbohydrate Polymers 67 (2007) 358–365
Carbohydrate Polymers
www.elsevier.com/locate/carbpol

Synthesis and characterization of chitosan-MMT biocomposite systems

Ebru Günister [a], Dilay Pestreli [a], Cüneyt H. Ünlü [b], Oya Atıcı [b,*], Nurfer Güngör [a]

[a] İ.T.Ü., Faculty of Science and Letters, Department of Physics, Maslak 34469, Istanbul, Turkey
[b] İ.T.Ü., Faculty of Science and Letters, Department of Chemistry, Maslak 34469, Istanbul, Turkey

Received 4 April 2006; received in revised form 30 May 2006; accepted 1 June 2006
Available online 21 July 2006

Abstract

Chitosan polymer was added to the montmorillonite (MMT) dispersions in different concentrations in the range of 1×10^{-2}–50×10^{-2} g/L (in 1% acetic acid solution). The rheological behaviours and colloidal properties of the clay dispersions were determined as a function of increasing polymer concentration. The studies on zeta potential measurements indicated that chitosan attached on the surface of clay particles. XRD analyses displayed that organic molecules did not enter enough sufficiently into the layers of clay structures. In the second part of the study, the rheological behaviour of 1 g/L chitosan dispersion in 1% acetic acid solution was investigated. Flow curves were analyzed using the Bingham model. The MMT/chitosan dispersions prepared at concentrations in a range of 1–50 g/g, and then rheological and electrokinetic measurements were repeated for these samples and studied together with the first measurements. The characterization with different methods (FTIR, AFM, DSC, and TGA) on chitosan-MMT biocomposite systems was examined.

Keywords: Chitosan; Biocomposite; Rheology; Zeta potential; Surface topology

1. Introduction

Smectite-group clay minerals have large adsorption capacities for polymer molecules due to their unique crystal structure. Montmorillonite is a member of the smectite group minerals and has a layered structure. The polymers in the montmorillonite dispersions interact with the clay particles, according to their ionic or non-ionic character. The ionic polymers induce electrostatic interactions, but the non-ionic polymers are adsorbed on the surface of clay minerals by the steric interactions. Polymer concentration, its molecular weight and hydrolyzing groups of polymer, size and shape of clay particle, its surface charge, clay concentration in suspension, pH, and temperature may all affect the clay/polymer interactions. The adsorption of polymers onto the surfaces of clay particles influences the rheologic and electrokinetic properties of the system. The effects of polymers on the montmorillonite dispersions are extensively studied (Alemdar, Güngör, Ece, & Atıcı, 2005a; Alemdar, Güngör, Ece, & Erim, 2005b; Billingham, Breen, & Yarwood, 1997; Chang, Gupta, & Ryan, 1992; Ece, Alemdar, Güngör, & Hayashi, 2002; Güngör & Karaoglan, 2001; Luckham & Rossi, 1999; Zhao, Urano, & Ogasawara, 1989). Recently, nanoscale composites of polymers with organo-clay have been studied extensively. Montmorillonite is the most widely used layered silicate in polymer nanocomposite. The use of clay in making nanocomposite has recently been increased because of the cheap and easy provide of it (Chang, Park, & Ihn, 2002; Chen & Curliss, 2003; Darder, Colilla, & Ruiz, 2005; İşci, Günister, Ece, & Güngör, 2004; Pinnavaia & Beall, 2000; Yang et al., 2003).

Chitosan is a polymer derived from chitin and is used in applications from health care to agriculture to dyes for fabrics. There are even medical applications. Chitosan itself is the major source of the nutritional supplement glucosamine. Chitosan is, at the pH of the gastrointestinal tract, a positively charged polymer and can bind to negatively charged substances. Chitosan might bind to some dietary lipids. It may also bind to the fat-soluble vitamins A, D,

* Corresponding author. Fax: +90 212 285 63 86.
E-mail address: atici@itu.edu.tr (O. Atıcı).

0144-8617/$ - see front matter © 2006 Elsevier Ltd. All rights reserved.
doi:10.1016/j.carbpol.2006.06.004

E, and K, as well as flavonoids, carotenoids, and some minerals, such as zinc, found in foods (Koide, 1998).

In this work, we investigate the effect of chitosan polymer on the rheological and colloidal properties of MMT dispersions at different chitosan concentrations and after the effect of MMT clay on the rheological and colloidal properties of chitosan biocomposite dispersions at different MMT concentrations. The structure analysis of chitosan/MMT biocomposite materials was studied using FTIR and AFM and the thermal behaviour of the biocomposite was determined using TGA and DSC.

2. Experimental

2.1. Materials

Natural bentonite sample was collected from Ünye area Eastern Black Sea coast of Turkey. It is labelled as MMT. Chitosan [400,000] was purchased from Fluka and used as received.

2.2. Preparation of chitosan/MMT and MMT/chitosan biocomposite systems

The first part of the experiment chitosan/MMT system was prepared. Four percentage MMT dispersion and 1 g/L chitosan was prepared in 1% acetic acid separately. Chitosan in 1% acetic acid were added to 4% MMT dispersions in 1% acetic acid at seven different concentrations in the range of 1×10^{-2}–50×10^{-2} g/L and obtained 2% chitosan/MMT biocomposite systems.

In the second part, the montmorillonite (MMT) was added to the chitosan dispersions (in 1% acetic acid solution) in 11 different ratios in the range of 1–50 [1, 2, 3, 4, 5, 6, 10, 20, 30, 40, 50 g/g (MMT/chitosan)].

2.3. Characterization of MMT, chitosan/MMT, and MMT/chitosan biocomposite systems

MMT has been identified as mainly smectite group minerals using X-ray diffraction (XRD) and FTIR analysis methods. XRD (Philips PW1140 model X-ray diffractometer) measurements were performed at room temperature on using Ni-filtered Cu-Kα radiation. FTIR analyses (400–4000 cm^{-1}) were performed on a Perkin-Elmer Spectrum One FTIR spectrometer using KBr pellets with a concentration of 1%. Spectral outputs were recorded either in absorbance or transmittance mode as a function of wave number. Chemical analyses were performed using a Perkin-Elmer 3030 model atomic absorption spectrophotometer. The sample had the chemical composition (wt%): SiO_2 70.30; Al_2O_3 15.00; Fe_2O_3 1.10; CaO 1.60; MgO 2.30; Na_2O 1.45; K_2O 1.20; TiO_2 0.30, ignition loss 6.45.

Particle size distribution was measured by using Micrometrics Model 5000D sedigraph, for sample dispersed in water, with calgon and subjected to magnetic stirring. The average particle sizes of sample have been found as 0.50 μm. The specific surface areas of the samples were determined by dye absorption technique. The calculated values of the specific surface are 120 m^2/g.

The flow behaviour of the dispersions was measured in a Brookfield DV-III type low-shear rheometer. The rheological behaviour of the clay suspensions was obtained by shear stress-shear rate measurements within 0–330 s^{-1} shear rates. Rheological measurements were carried out in duplicate.

The zeta potential measurements were carried out using a Malvern Instruments, Zetasizer 2000. The optic unit contains a 5 mW He–Ne (638 nm) laser. Before the measurements, all the dispersions were centrifuged at 4500 rpm for 30 min. Supernatants were then used for zeta potential measurements.

The thermogravimetric analysis (TGA) was done on a TGA Q50 V6.3 Build 189 with the heating rate of 20 °C/min under N_2 atmosphere. Differential scanning calorimeter (DSC) was used on a DSC Q10 V8.1 Build at a heating rate of 10 °C/min.

Digital Instruments, SPM-9500J3 SHIMADZU Scanning Probe Microscope was used to examine the surface topology.

3. Results and discussion

3.1. Rheologic and electrokinetic studies of chitosan/MMT and MMT/chitosan biocomposites

The rheologic characterization of the MMT was examined. The flow and apparent viscosity-shear velocity curves of the 1%, 2%, 3%, 4%, 5%, and 6% of dispersions that have been prepared with the MMT sample, have been drawn and the flow models are determined. The shear stress versus shear rate for suspensions containing different concentrations of the MMT samples are shown in Fig. 1. All the dispersions of the MMT exhibited Newtonian

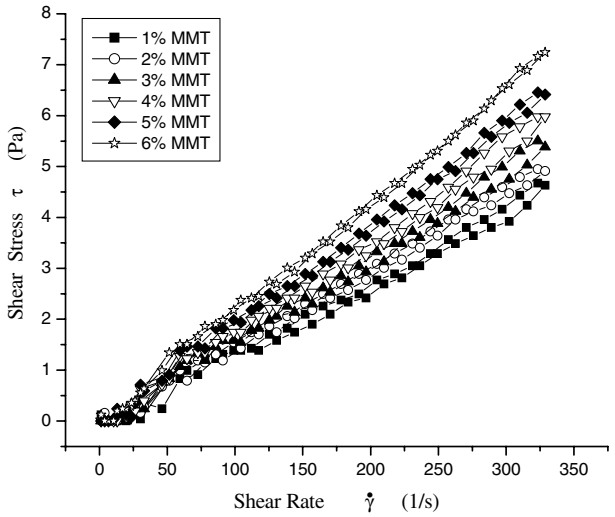

Fig. 1. The effect of clay concentration on the flow curves.

behaviour. Yield value has not found. Because the yield value could not be found we can say that the interaction between the particles at this dispersion is very small. The electrophoretic mobility and zeta potential value was 3.33 μm cm/V s, −42.4 mV for MMT dispersions (2 w/w %), respectively. This value displays deflocculating structure of dispersion. The zeta potential is an indicator of pushing between the particles.

The effects of chitosan on MMT dispersions (2 w/w %) were investigated in detail using electrokinetic parameters, such as mobility and zeta potentials (Fig. 2), and rheologic parameters, such as viscosity, yield value, apparent and plastic viscosity (Fig. 3a and b). Fig. 2 shows the variations in the zeta potential as a function of the concentrations of the chitosan. The zeta potential value unadulterated with polymer the MMT + 1% acetic acid dispersion has been measured as −5 mV. This value determines the system displaying a flocculate structure. As can be seen, zeta potential values decrease in absolute value with increasing the concentration of chitosan. It is observed that the cationic polymer was held by clay surface. The decrease on the zeta potential revealed that positively charged chitosan molecules attached on the negatively charged clay particles. The zero point of charge (isoelectric point) of the chitosan/MMT biocomposite particles was observed at 0.2 g/L.

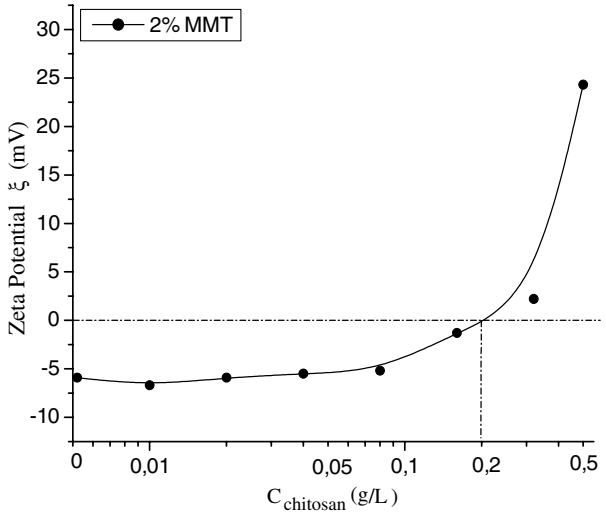

Fig. 2. The variation of the zeta potential versus chitosan concentration for 2% w/w MMT + 1% acetic acid dispersion.

The dispersions of MMT + 1% acetic acid systems exhibit Bingham plastic flow behaviour. Yield value was found very small. First, it was observed that the viscosity and yield value increased slightly with increasing amount of chitosan added. Maximum apparent viscosity is observed of 7.44 m Pa s at 0.32 g/L chitosan. It is observed that flow model of 2% MMT dispersion did not change until the addition of 0.50 g/L chitosan. With the last chitosan addition (0.5 g/L) to the MMT dispersions, the decrease in rheological parameters has been determined (Fig. 3a and b). After this addition, the flow of dispersion can be defined as nearly Newtonian. Yield value has not been found. The sharp increase after that concentration is attributed to a decrease in the particle surface charge of the clay with the adsorption of oppositely charged chitosan and also bridge action of chitosan between clay particles (Alemdar et al., 2005a, 2005b; Tadros, 1987). The groups existing before the addition have been dispersing and the environment can display less resistant against the flow. These results are in good agreement with the behaviour of zeta potential of MMT dispersion (Fig. 2).

Fig. 4 was shown schematically representation of interaction of chitosan polymer with MMT particles. The positive charged chitosan has been interacting with the negative charged clay particles, the clay particle surfaces had been covered by chitosan by increasing the concentration of chitosan. The graph has been plotted according to the results of rheological and electrokinetic measurements.

In the second part of the study, we investigate the effect of MMT on the rheological, colloidal and morphologic, structural properties of 1 g/L chitosan dispersion in 1% acetic acid solution dispersions different MMT concentrations. A value of 1 g/L chitosan + 1% acetic acid dispersions exhibit Bingham plastic flow behaviour. Yield value was found very small (0.33 Pa). The MMT samples ranging

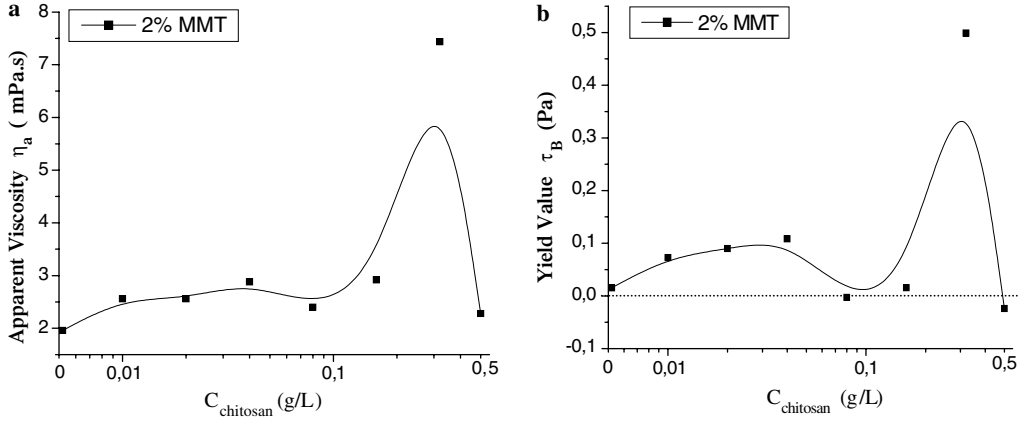

Fig. 3. The changes of the rheological parameters of MMT dispersions with chitosan polymer added to dispersions; (a) apparent viscosity, (b) yield value.

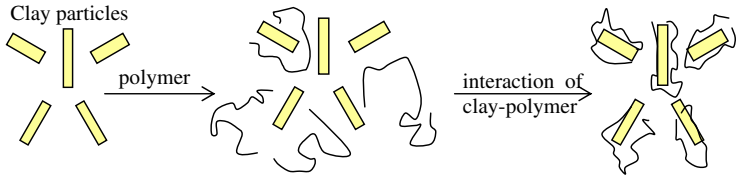

Fig. 4. Schematic representation of interaction of chitosan polymer with MMT particles.

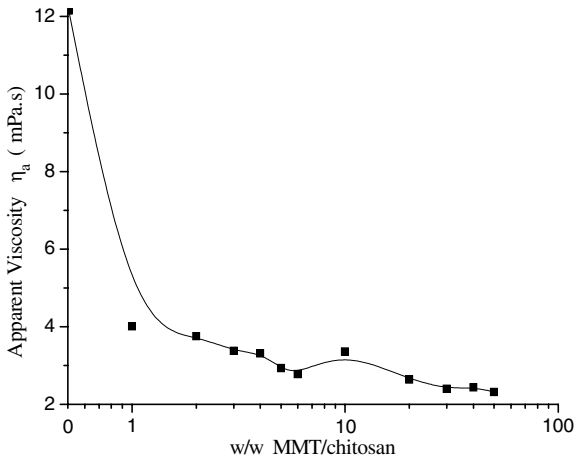

Fig. 5. The changes of the apparent viscosity of chitosan + 1% acetic acid dispersions with MMT clay added to dispersions.

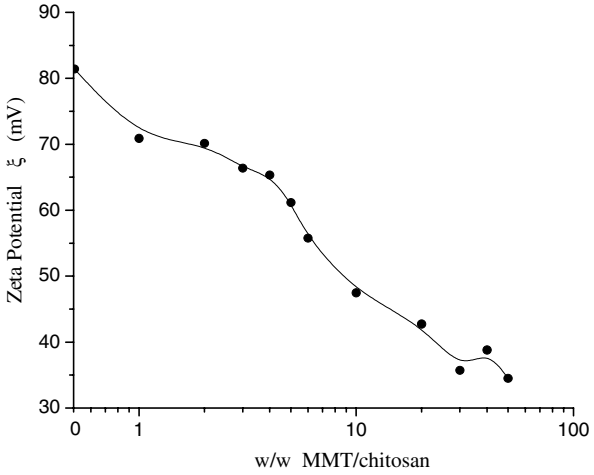

Fig. 6. The changes of the zeta potential of chitosan + 1% acetic acid dispersions with MMT clay added to dispersions.

between 1 and 50 g/g concentrations were added to the chitosan dispersion (Fig. 5), as called MMT/chitosan biocomposite. The rheologic and electrokinetic measurements have indicated that the environment has displayed a more defloccule structure by the increase of the bentonite amount. Except the dispersion which has a 50 g/g (MMT/chitosan) ratio, all dispersions has been displayed a Newtonian flow. Only a little yield value (0.014 Pa) has been determined at the dispersion that has a 50 g/g (MMT/chitosan) ratio (Fig. 5). The rheological parameters became small by the addition of MMT to the chitosan dispersions; the clay particles have caused the decrease in the resistance of polymer against the flow. The negative charged clay particles have been interacting with the positive charged polymer electrostatically, by attaching them to its surface, obtaining the environment flow easily.

The zeta potential value of 1% chitosan solution has been measured as +86.6 mV. Increase in the concentration of the montmorillonite further results in a decrease on the zeta potential value of the chitosan dispersion. This decrease on the zeta potential revealed that positively charged polymer molecules attached on the negatively charged clay particles. The zeta potential decreases with increasing concentration of MMT in MMT/chitosan systems. This is the evidence of the interaction between polymer molecules and net negative load carrying clay particles (Fig. 6).

Fig. 7 gives schematic representation of interaction of chitosan + 1% acetic acid polymer with MMT clay added to dispersions. The environment at the figure has been designed as a dispersion which has separate clusters of structures and consists of polymer molecules that interact with clay particles.

3.2. Spectral studies of chitosan/MMT and MMT/chitosan biocomposites

In order to understand whether added chitosan enters into the interlayer of clay minerals or not, XRD analyses were done to measure d-spacing (Fig. 8). It is clear that peak position (d-spacing) in X-ray data must move to smaller angles for the wider interlayer distance in the modified clay. The d-spacing for the unmodified MMT was found at $2\theta \approx 7°$, which corresponds to an interlayer distance of 12.6 Å (Fig. 8a). When the addition of acetic acid (1% and 10% concentrations) to the aqueous dispersions of MMT, the increased the d-spacing of modified clay was found at $2\theta = 5.85°$, corresponding to an interlayer distance of 15.09 Å (Fig. 8b and c). On the other hand, X-ray diffraction data for both chitosan/MMT and MMT/chitosan biocomposites exhibited the d-spacing in the relevant region (Fig. 8d and e); indicating maximum interlayer distances 16.34 Å ($2\theta = 5.4°$). So, XRD analyses results indicate that chitosan molecules did not enter sufficiently into the layers of clay structures.

The structure of the chitosan biocomposite particles was analyzed by using FTIR spectroscopy. Fig. 9a–c shows FTIR spectra of MMT/chitosan biocomposites and MMT dispersions. The spectrum of MMT shows the

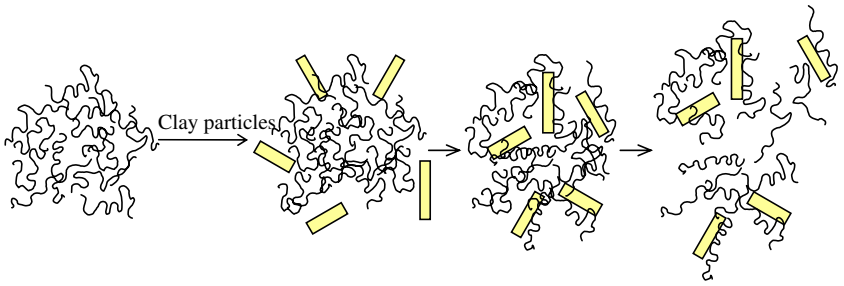

Fig. 7. Schematic representation of interaction of chitosan + 1% acetic acid polymer with MMT clay added to dispersions.

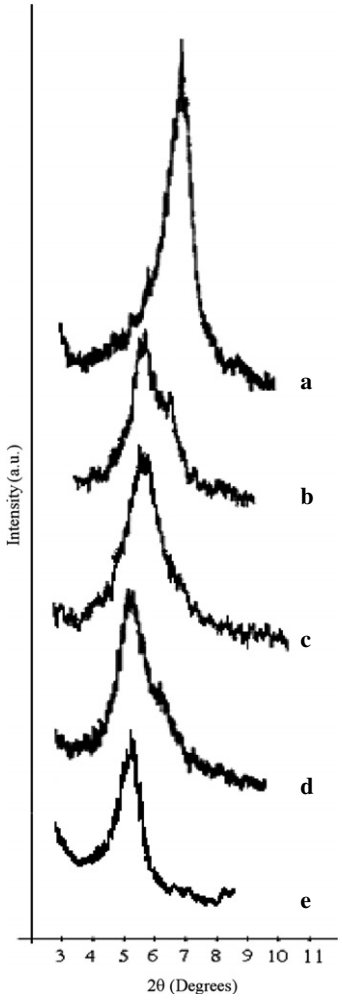

Fig. 8. XRD data of 2% MMT dispersed in (a) distillated water, (b) 1% acetic acid, (c) 10% acetic acid, and (d) 2% MMT dispersion with 0.08 g/L chitosan in 1% acetic acid, (e) 6 g/g (MMT/chitosan) dispersion in 1% acetic acid.

characteristic bands 3627 cm^{-1} due to O–H stretching, a broad peak centred on 3449 cm^{-1} due to interlayer and intralayer H-bonded O–H stretching, 1641 cm^{-1} due to H–O–H bending, 1087 and 1035 cm^{-1} due to Si–O stretching, 916 and 626 cm^{-1} due to Al–OH, 843 and 793 cm^{-1} due to (Al, Mg)–OH vibration modes and 520 and 467 cm^{-1} due to Si–O bending vibrations (Alemdar et al., 2005a; Marel & Beutelspacher, 1976). The exchange of simple inorganic cations by the other ions results in the enhancement of the intensity of the 3500–3200 cm^{-1} band along with a reduction of intensities due to Si–O and Al–O. The increase in intensity of the 3500–3200 cm^{-1} band reflects the increased hydrogen bonding between the lattice hydroxyls and organic groups. When the protons in chitosan are hydrogen-bonded to the oxygen species of Si–O and Al–O segment, Si–O and Al–O bonds would be weakened and the tetrahedral symmetry of these moieties will be distorted. On the other hand, FTIR analysis shows that the MMT/chitosan composites exhibited resolved N–H, O–H, and C–H bands when the composites are formed. The chitosan composites show three stretching vibration regions: N–H and O–H from chitosan, and O–H, Si–O, (Al, Mg)–OH, or Al–OH from the MMT. This would result in the change of the IR band positions as well as the reduction of intensities of the bands. It can clearly be seen that the chitosan adsorbed MMT spectra; exhibit the presence of characteristic absorptions due to the organic and inorganic groups.

While standard chitosan showed peaks at 2929 and 2874 cm^{-1} (aliphatic C–H stretching), 1385 cm^{-1} (C–H bending), 1651 cm^{-1} (N–H bending), 1560 cm^{-1} (N–H bending), 1425 and 1401 cm^{-1} (C–H bending), 1138 and 1095 cm^{-1} (C–O stretching), and the infrared spectra of 10 g/g (MMT/chitosan) biocomposite (Fig. 9a) showed additional peaks including 1612 cm^{-1} (N–H bending), 1566 cm^{-1} (N–H bending), 1450 and 1425 cm^{-1} (C–H bending), and also absorbencies due to structural O–H stretching at 3621 cm^{-1}, H–O–H deforming (absorbed water) at 1634 cm^{-1}, and Al–O vibrations at 915, 624 842, and 792 cm^{-1} confirm the presence of MMT in the dispersion. In the bentonite chitosan adsorption products, the structural O–H stretching peak was broadened and gave a maximum at 3621 cm^{-1}, and the Si–O stretching peaks were also gave a maximum at 1086 and 1034 cm^{-1} and finally Si–O bending peaks were not changed significantly (520 and 467 cm^{-1}). The spectrum of 50 g/g (MMT/chitosan) biocomposite also contains characteristic bands of all components. These results showed that the chitosan molecules and clay particles mainly interact on the surface each other. The O–H stretching frequencies of the MMT-chitosan biocomposite molecules adsorption products were broadened and displaced to lower frequencies by about 12–14 cm^{-1}. These shifts may be attributed to formation hydrogen bonds. In addition, the intensities of the Al–O

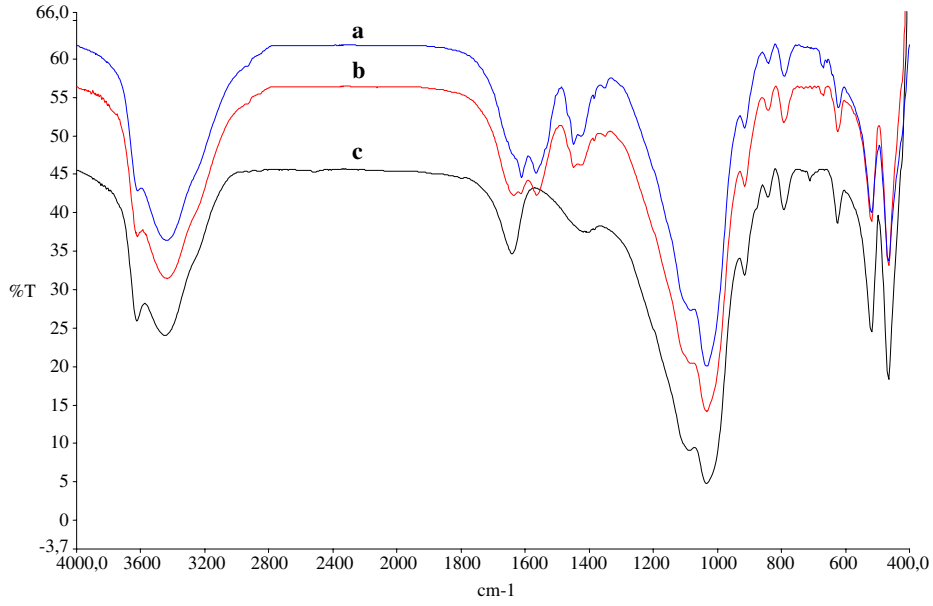

Fig. 9. FTIR spectra of (a) 10 g/g (MMT/chitosan) dispersions, (b) 50 g/g (MMT/chitosan) dispersions, (c) Na-montmorillonite.

bands and structural O–H stretching vibrations also decrease in the order MMT < 50 g/g (MMT/chitosan) < 10 g/g (MMT/chitosan). This is attributed to the relaxation of hydrogen bonding between (Al–O) O–H deformations as well as to the hydrated water of exchangeable cationic metal ions on the montmorillonite surface. This observation is in agreement with our explanation of the change in zeta potential and XRD studies.

3.3. Morphology of biocomposites

Atomic Force Microscopy technique was used to characterize the morphology of MMT/chitosan biocomposite systems. Fig. 10a and b shows, AFM image of the surface of 10 g/g (MMT/chitosan) and 50 g/g (MMT/chitosan), respectively. When a layered structure has been observed at Fig. 10a, the clusters formed of layered structures by increasing the clay particles (Fig. 10b). The average dimensions of the clusters have been determined approximately 2.2 μm. The mean surface roughness, R_a, of the samples was measured with scanning areas of $5.00 \times 5.00\ \mu m^2$. R_a values are; 205.5 nm for 10 g/g (MMT/chitosan) biocomposite film, 177.5 nm for 50 g/g (MMT/chitosan) biocomposite film.

3.4. Thermal properties of biocomposites

Table 1 shows the TGA and DSC results for pure chitosan, 10 and 50 g/g (MMT/chitosan) biocomposite. It was found that the MMT/chitosan biocomposite particles

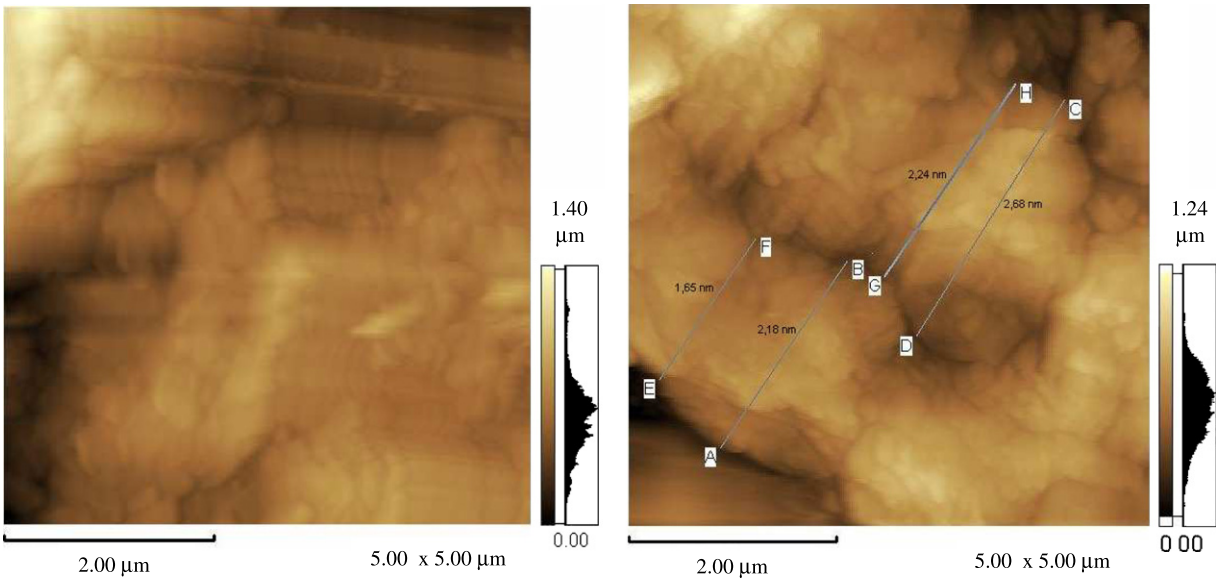

Fig. 10. Atomic force microscopy image of (a) 10 g/g (b) 50 g/g (MMT/chitosan) dispersions.

Table 1
TGA and DSC analysis results

Material	T_B^{20}[a] (°C)	T_D^{max}[b] (°C)	W_R^{600}[c] (%)	T_g[d] (°C)	T_m[e] (°C)
Chitosan	279	718	35	50	137
MMT/chitosan (10 g/g)	666	727	81	Not observed	152
MMT/chitosan (50 g/g)	431	687	76	149	226

[a] Twenty percentage weight loss onset temperature.
[b] Maximum weight loss onset temperature.
[c] Weight percent of residue at 600 °C.
[d] Glass-transition temperature.
[e] Melting temperature.

exhibited a higher thermal decomposition temperature compared to pure chitosan particles. Because inorganic species have good thermal stabilities, it is generally believed that the introduction of inorganic components into organic materials can improve their thermal stability. This increase in the thermal stability can be attributed to the high thermal stability of clay and to the interaction between the clay particles and the chitosan (Chang, An, & Sur, 2003; Strawhecker & Manias, 2000). Twenty percentage weight loss of chitosan, 10 g/g MMT/chitosan, and 50 g/g MMT /chitosan was observed as 279, 666, and 431 °C, respectively. Maximum weight loss percentages for chitosan, 10 and 50 g/g (MMT/chitosan) composites were observed as 718 °C (weight loss 65%), 727 °C (weight loss 19%), and 687 °C (weight loss 24%), respectively. Weight of the residue at 600 °C increased with clay loading. In brief, the thermal stability of chitosan-MMT biocomposite was observed to increase with 91% clay content (10 g/g (MMT/chitosan) biocomposite). This implies that MMT was effective in improving the thermal stability of the chitosan systems.

The glass-transition behaviours of the chitosan and MMT/chitosan biocomposite systems were measured by the DSC analysis. The glass transition temperature and melting endothermic peak of chitosan, 10 g/g (MMT/chitosan), and 50 g/g (MMT/chitosan) has been shifted remarkably. Compared the glass transition temperature of chitosan and 50 g/g MMT, the temperature is shifted from 50 to 149 °C. DSC does not detect any traces of thermal transitions for between 10 g/g MMT/chitosan. The melting endothermic peak of chitosan is observed at 137 °C, while the peak of 10 g/g (MMT/chitosan), 50 g/g (MMT/chitosan) biocomposites is shown at 152 and 226 °C, respectively. The melting temperature increased with increasing amounts of clay in the chitosan.

4. Conclusion

The adsorbed chitosan are affected the rheological, electrokinetic, and surface properties of MMT dispersions. The electrokinetic measurements have shown that the chitosan polymer stays on the clay particle surfaces and the XRD studies have shown that they do not get into the basal intervals. The FTIR spectra can clearly be seen that all spectra exhibit the presence of characteristic absorptions due to the organic and inorganic groups. FTIR results show that the chitosan molecules and clay particles mainly interact on the surface each other. The surface of the 10 g/g (MMT/chitosan) biocomposite films is rougher than that of the 50 g/g (MMT/chitosan) biocomposite film.

The rheologic measurements have displayed that the chitosan addition to montmorillonite dispersions has caused first flocculation then deflocculating in the dispersion. However, when clay addition is made to chitosan, the system has become deflocculated from the first addition. When the clay amount is increased the thermal tenacity of chitosan has been increased. As a result if deflocculated structure of chitosan is desired and a higher thermal tenacity is asked for, the addition of montmorillonite will give positive results.

Acknowledgements

This paper is supported by Research Fund of Istanbul Technical University, Turkey (Project No: 1229). The authors thank Prof. Dr. Fatma Tepehan and Mr. Esat Pehlivan for AFM measurements, and Prof. Dr. Ö. Işık Ece for XRD spectrum measurements.

References

Alemdar, A., Güngör, N., Ece, Ö. I., & Atıcı, O. (2005a). The rheological properties and characterization of bentonite dispersions in the presence of non-ionic polymer PEG. *Journal of Materials Science, 40*, 171–177.

Alemdar, A., Güngör, N., Ece, Ö. I., & Erim, F. B. (2005b). Effects of polethyleneimine adsorption on the rheological properties of purified bentonite suspensions. *Colloids and Surfaces A-Physicochemical and Engineering Aspects, 252*, 95–98.

Billingham, J., Breen, C., & Yarwood, J. (1997). Adsorption of polyamine acid and polyethylene glycol on montmorillonite: an in situ study using ATR-FTIR. *Vibrational Spectroscopy, 14*, 19–34.

Chang, S. H., Gupta, R. K., & Ryan, M. E. (1992). Effect of the adsorption of polyvinyl alcohol on the rheology and stability of clay suspensions. *Journal of Rheology, 36*(2), 273–287.

Chang, J. H., Park, D. K., & Ihn, K. J. (2002). Polimide nanocomposite with a hexadecylamine clay: synthesis and characterization. *Journal of Applied Polymer Science, 84*, 2294–2301.

Chang, J. H., An, Y. U., & Sur, G. S. (2003). Poly(lactic acid) nanocomposites with various organoclays. I. Thermomechanical properties, morphology, and gas permeability. *Journal of Polymer Science Part B: Polymer Physics, 41*, 94–103.

Chen, C., & Curliss, D. (2003). Processing and morphological development of montmorillonite epoxy nanocomposites. *Nanotechnology, 14*, 643–648.

Darder, M., Colilla, M., & Ruiz, H. E. (2005). Chitosan-clay nanocomposites: application as electrochemical sensors. *Applied Clay Science, 28*, 199–208.

Ece, Ö. I., Alemdar, A., Güngör, N., & Hayashi, S. (2002). Influences of non-ionic poly(ethylene glycol) polymer PEG on electrokinetic and rheological properties of bentonite suspensions. *Journal of Applied Polymer Science, 86*, 341–346.

Güngör, N., & Karaoglan, S. (2001). Interactions of polyacrylamide polymer with bentonite in aqueous systems. *Materials Letters, 48*, 168–175.

İşci, S., Günister, E., Ece, Ö. I., & Güngör, N. (2004). The modification of rheologic properties of clays with PVA effect. *Materials Letters, 58*, 1975–1978.

Koide, S. S. (1998). Chitin-chitosan: properties, benefits and risks. *Nutrition Research, 8:6*, 1091–1101.

Luckham, P. F., & Rossi, S. (1999). The colloidal and rheological properties of bentonite suspensions. *Advances in Colloid and Interface Science, 82*, 43–92.

Marel, H. W., & Beutelspacher, H. (1976). *Atlas of infrared spectroscopy of clay minerals and their mixtures*. Amsterdam: Elsevier Scientific.

Pinnavaia, T. J., & Beall, G. W. (2000). *Polymer-clay nanocomposites*. New York: John Wiley& Sons Ltd.

Strawhecker, K. E., & Manias, E. (2000). Structure and properties of poly/vinyl alcohol/Na montmorillonite nanocomposites. *Chemistry of Materials, 12*, 2943–2949.

Tadros, Th. F. (1987). *Solidlliquid dispersions*. London: Academic Press.

Yang, F., Zhang, X., Zhao, H., Chen, B., Huang, B., & Feng, Z. (2003). Preparation and properties of polyethylene/montmorillonite nanocomposites by in situ polymerization. *Journal of Applied Polymer Science, 89*(13), 3680–3684.

Zhao, X., Urano, K., & Ogasawara, S. (1989). Adsorption of polyethylene glycol from aqueous solution on montmorillonite clays. *Colloid and Polymer Science, 267*, 899–906.